Received: 13 October 2022 | Revised: 5 December 2022 | Accepted: 20 December 2022

DOI: 10.1111/1556-4029.15190

JOURNAL OF FORENSIC SCIENCES AAFS

ORIGINAL PAPER

Criminalistics

Linking ammonium nitrate-aluminum (AN-AL) post-blast residues to pre-blast explosive materials using isotope ratio and trace elemental analysis for source attribution

Paul Ippoliti MS[1] | Jeffrey Werlich BS[1] | Cami Fuglsby MS[2] | Chris Yarnes PhD[3] | Christopher P. Saunders PhD[2] | Josh Dettman PhD[1]

[1]MIT Lincoln Laboratory, Lexington, Massachusetts, USA

[2]South Dakota State University, Brookings, South Dakota, USA

[3]University of California, Davis, California, USA

Correspondence
Josh Dettman PhD, MIT Lincoln Laboratory, 244 Wood Street, Lexington, MA 02421, USA.
Email: joshua.dettman@ll.mit.edu

Funding information
National Institute of Justice Interagency Agreement, Grant/Award Number: DJO-NIJ-19-RO-0002-2

Abstract

Forensic science practitioners are often called upon to attribute crimes using trace evidence, such as explosive remnants, with the ultimate goal of associating a crime with a suspect or suspects in order to prevent further attacks. The explosive charge is an attractive component for attribution in crimes involving explosives as there are limited pathways for acquisition. However, there is currently no capability to link an explosive charge to its source via post-blast trace residues using isotope ratios or trace elements. Here, we sought to determine if pre-blast attribution signatures are preserved after detonation and can be subsequently recovered and detected. A field study was conducted to recover samples of post-blast explosives from controlled detonations of ammonium nitrate-aluminum (AN-Al), which were then analyzed via isotope ratio mass spectrometry (IRMS) and inductively coupled plasma-mass spectrometry (ICP-MS) for quantitation and profiling of isotopes ratio and trace element signatures, respectively. Oxygen and nitrogen isotope ratios from AN-Al yielded some of the most promising results with considerable overlap within one standard deviation of the reference between the spreads of pre- and post-blast data. Trace element results from AN-Al support the findings in the isotope ratio data, with 26 elements detected in both pre- and post-blast samples, and several elements including B, Cd, Cr, Ni, Sn, V, and Zn showing considerable overlap. These preliminary results provide a proof-of-concept for the development of forensic examinations that can attribute signatures from post-blast debris to signatures in pre-blast explosive materials for use in future investigations.

KEYWORDS
elemental analysis, explosives, forensic science, inductively coupled plasma-mass spectrometry (ICP-MS), isotope ratio mass spectrometry (IRMS), post-blast

Highlights

- Identification of pre-blast AN-Al signatures was possible after detonation
- Isotope ratio mass spectrometry yielded the most promising results of all techniques explored
- ICP-MS yielded twenty-six elements with seven elements showing overlap between pre- and post-blast

1 | INTRODUCTION

Post-blast investigations are conducted by domestic law enforcement, defense, and intelligence organizations to generate leads in high-profile terrorism cases involving the detonation of explosives. The ultimate goal of these investigations is to find evidence to associate the explosive attack with a suspect or suspects, otherwise known as post-blast attribution. This is important for the prevention of further attacks through exclusion, exoneration, arrest, and criminal prosecution of potential perpetrators. To enable attribution of the attack, investigators piece together a history of the events preceding the attack in an attempt to find a link between the attack and potential suspects. This includes collecting remaining fragments of the explosive device, determining the source (i.e., distributor or original manufacturer) of the recovered components, and potentially identifying suspects through associations with the identified component source, for example, by surveillance, receipts, or Internet search history.

Among the potential recovered components of a device, the explosive charge is an attractive component for attribution as it is key to the functioning of the device and there are limited pathways for acquisition. However, unlike pre-blast attribution where there is some limited capability to compare signatures from an unexploded device to manufacturer reference samples, there is currently no capability to link the explosive charge to its source via post-blast trace residues. Attributing the explosive post-blast is a challenge because very little explosive material remains after detonation. In addition, the detonation process and subsequent environmental exposure can result in physical or chemical changes to explosives properties during and after detonation. Developing a post-blast attribution capability would enhance the ability of investigators to tie the crime to potential suspects.

Prior work at Massachusetts Institute of Technology—Lincoln Laboratory (MITLL) examined multiple signatures from ammonium nitrate fertilizer prills such as trace elements, color, and morphology. Most published applied research efforts for attribution have focused on using isotope ratio mass spectrometry (IRMS) to compare pre-blast explosives and their precursors to a suspected source [1]. This technique has been used to differentiate commercial/military grade explosives such as 2,4,6-trinitrotoluene (TNT) [2], pentaerythritol tetranitrate (PETN) [3, 4], Semtex [5], black powder [6], 1,3,5-trinitro perhydro-1,3,5-triazine (RDX) and 1,3,5,7-tetranitro-1,3,5,7-tetrazo cane HMX [3], as well as improvised explosives and their precursors such as ammonium nitrate [4, 7–10], hydrogen peroxide [11], urea nitrate [12], and triacetone triperoxide (TATP) [4, 13]. Other work has also demonstrated the use of inductively coupled plasma-mass spectrometry (ICP-MS) for trace element analysis of signatures in pre-blast investigations [9, 14]. High performance liquid chromatography mass spectrometry (HPLC-MS) has also been used extensively for the identification of organic explosive compounds including TNT, RDX, HMX, and PETN from post-blast sites [15–17]. In addition to the explosive compound itself, other organics found in certain explosive materials such as binders, plasticizers, and other additives [18] can potentially act as useful signatures detectable by HPLC-MS. Some work on post-blast explosive attribution has been done, but it has been limited to a few studies [4, 19]. McGuire et al. [19] obtained $\delta^{13}C$ values for aromatic explosives that were consistent pre- and post-blast, but isotopic fractionation was observed for ^{13}C for non-aromatic explosives and ^{2}H and ^{15}N fractionation in all explosives tested. Benson et al. [4] found that AN, both as commercial emulsions and improvised fuel oil mixtures, had a significant enrichment of ^{15}N post-blast, potentially due to exchange with atmospheric nitrogen caused by blast kinetic energy and environmental contamination/isotopic fractionation by soil microbe metabolism.

The purpose of this study was to determine if relevant conserved signatures characteristic of the origin/source of an explosive can be recovered post-blast and matched to pre-blast signatures. To test this hypothesis, a field experiment was designed to conduct replicate detonations of multiple types of explosive materials, followed by collection of post-blast residue. The samples of post-blast residue were then processed and analyzed via multiple analytical techniques to acquire signatures that may be specific to the explosive source. The signatures from post-blast samples were statistically compared with signatures from pre-blast samples to determine if they were preserved. For the purposes of this research article, only methods and results for AN-AL tests will be discussed. While tests for RDX and TNT were conducted, the amount of post-blast residue recovered was either not detected at all by the analytical instrumentation, or too few samples yielded quantifiable results to draw any reasonable conclusions.

2 | MATERIALS AND METHODS

2.1 | Field test design and execution for realistic sample generation

2.1.1 | Field test design

Three explosive types were chosen as part of this study: RDX, TNT, and AN-Al as relevant explosives encountered in investigations, although only methods relevant to AN-AL will be discussed here. The main design criteria for the test were to be as operationally relevant as possible by conducting the explosive detonations and sample collections in an open, outdoor environment as opposed to a laboratory setting. The field experiments were conducted at an explosives test range in Edgefield, SC. The test grid was divided into four quadrants with each quadrant designated for a specific explosive type. Cross-contamination mitigation measures included conducting tests for the different explosive types in separate locations on the test grid, raising the explosive charges two meters off the ground, placing a 10×10 m tarp on the sample grid, and dousing the grid with water between each detonation. The explosive charges were prepared in $2'' \times 10.5''$ acrylic cylindrical tubes and approximately 1 pound of explosive was used per shot for each of the explosive types.

The sampling grids for all detonations were arranged in concentric circles at 3 and 5 m from the center, with large (six inch)

polystyrene dishes placed every 30° as seen in Figure 1. In total, there were 27 sample collection sites for each detonation, with 4 replicate detonations for each explosive type. In addition to post-blast samples, there were four cross-contamination dishes (CCD) on the grid, which were placed at the start of each grid setup or post-blast sampling collection and collected at the end of each session to determine if any explosive was kicked up by personnel during setup or sampling.

2.1.2 | Sample grid setup

A typical sample grid setup began with wetting the blast area and centering a tarp beneath the suspended explosive charge. Metal plates with Velcro were placed at each of the sample locations shown in Figure 1, followed by placement of the four cross-contamination dishes. Clean sample dishes with Velcro on the bottom, were then placed on the metal plates. All samples were placed using the clean hands, dirty hands method described in Environmental Protection Agency (EPA) Method 1669 [20]. The "dirty hands" sampler (DH) handles all materials that may potentially be contaminated. The "clean hands" sampler (CH) dons a clean pair of gloves between every sample and places the appropriate sample collection device. Once sample grid setup was completed, the cross-contamination samples were collected before leaving the grid. Positive and negative control samples were located off the sample grid, which were then placed once the sample grid was set up. Positive controls were made by placing approximately 5 mg of AN-AL on a dish. Negative controls were prepared by placing clean coupons or dishes next to the positive controls.

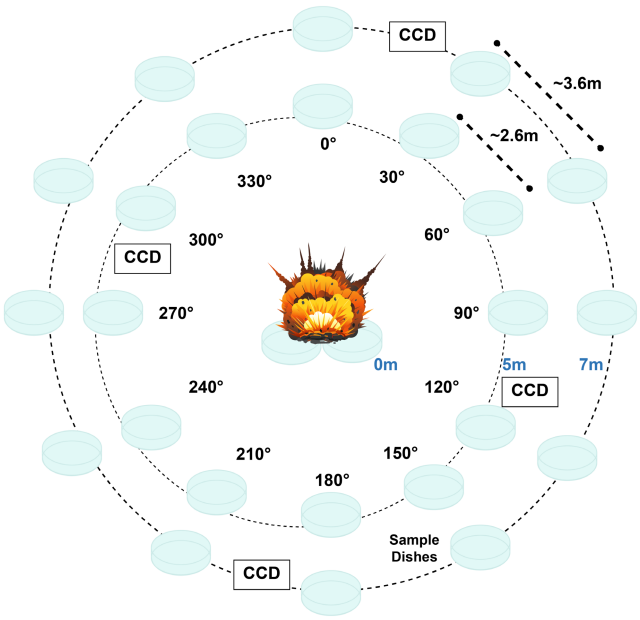

FIGURE 1 Example sample grid for an AN-AL detonation with polystyrene dishes arranged in concentric circles at 3 and 5 m from the center [Colour figure can be viewed at wileyonlinelibrary.com]

2.1.3 | Sample collection

All methods for handling and collecting post-blast samples were adapted from the environmental or forensic science literature including the "clean hands, dirty hands" approach described in EPA Method 1669 [20], as well as support from other sources in the literature [21, 22]. After a detonation, sampling began by collecting the positive and negative control samples and placing clean cross-contamination dishes on the sample grid, followed by collecting all post-blast samples as described in the above referenced methods. Briefly, the DH handles all of the potentially contaminated materials while the CH handles all sterile materials and performs the sampling tasks. The lids of the polystyrene dishes were placed on top of the sample dishes, removed from the metal plates, and sealed with lab tape. Once all samples were collected, the cross-contamination samples were collected, followed by preparations for the next detonation.

2.1.4 | Sample extraction

AN-Al samples were extracted from the large polystyrene dishes by adding 5.6 ml of deionized water. The water extract was then transferred to a 15 ml tube and vortexed for 30 s. Next, 1 ml of each sample was transferred to HPLC vials for nitrate IRMS analysis. For trace elements analysis by ICP-MS, 200 µl of nitric acid and 200 µl of hydrochloric acid were added to the remaining sample in the 15 ml conical tube. The samples were then allowed to digest at room temperature overnight, followed by the addition of 8.6 ml deionized water the next morning.

2.2 | Instrumental methods for chemical signature collection

2.2.1 | ICP-MS quantitation

Extracted and digested AN-Al samples in dilute nitric and hydrochloric acids were analyzed for total aluminum content by ICP-MS using an Agilent 7900 ICP-MS (Agilent Technologies; Santa Clara, CA, USA). First, all samples were diluted 100 times in 2% each nitric and hydrochloric acid. External aluminum calibration standards were used for quantitation. The 30 samples with the highest concentrations of aluminum were selected and the 1 ml portions that were set aside for IRMS analysis. Note, the known amount of Al in the device prior to detonation is 8% by mass.

2.2.2 | Stable isotope analysis of ^{15}N and ^{18}O from ammonium nitrate

Purified nitrate samples were prepared for stable isotope analysis using the bacterial denitrifier method [23, 24] to convert sample

nitrate to nitrous oxide. Following conversion of sample nitrate to nitrous oxide, isotope ratios of ^{15}N and ^{18}O were measured using a Thermo Finnigan GasBench/PreCon trace gas concentration system interfaced to a Thermo Scientific Delta V Plus IRMS (Bremen, Germany). Gas samples were purged from vials through a double-needle sampler into a helium carrier stream (25 ml/min). The gas sample passed through a CO_2 scrubber (Ascarite) and N_2O was trapped and concentrated in two liquid nitrogen cryo-traps operated in series such that the N_2O was held in the first trap until the non-condensing portion of the sample gas had been replaced by helium carrier, then passed to a second, smaller trap, for cryofocusing. Finally, the second trap was warmed to ambient temperature and the N_2O was carried by helium to the IRMS following resolution of N_2O from residual CO_2 on an Agilent GS-Q capillary column (30 m × 0.32 mm, 40°C, 1.0 ml/min).

A reference N_2O peak was used to calculate provisional isotope ratios of the sample N_2O peak. Final $\delta^{15}N$ and $\delta^{18}O$ values were calculated by adjusting the provisional values such that calibrated $\delta^{15}N$ and $\delta^{18}O$ values for laboratory reference materials were obtained. All laboratory reference materials were directly traceable to the international reference scale for ^{15}N (Air) and ^{18}O (V-SMOW) through regular calibration using certified reference material nitrates USGS 32 (KNO_3; 180‰), USGS 34(KNO_3; −1.8‰), and USGS 35($NaNO_3$; 2.7‰), supplied by National Institute of Standards and Technology (NIST; Gaithersburg, MD USA). Additional laboratory reference materials were included in each batch to monitor and correct for instrumental drift and linearity. Mean analytical accuracy and precision of two quality control reference materials (KNO3) were ±0.07 and 0.18‰ for $\delta^{15}N$, and ±0.18 and 0.57‰ for $\delta^{18}O$, respectively. Precision and accuracy of all reference materials and sample technical replicates was better than ±0.4‰ for $\delta^{15}N$ and ±0.5‰ for $\delta^{18}O$ for nitrate concentrations from 4–7000 μM.

2.2.3 | ICP-MS profiling of AN-Al

Once AN-Al samples were quantified for total aluminum, ICP-MS analysis was conducted again using an Agilent 7900 ICP-MS (Agilent Technologies; Santa Clara, CA, USA) on the samples without any dilution to get the full profile of elements. The following isotopes/elements were monitored: 7 Li, 9 Be, 11 B, 23 Na, 24 Mg, 31 P, 34 S, 39 K, 44 Ca, 47 Ti, 51 V, 52 Cr, 55 Mn, 56 Fe, 59 Co, 60 Ni, 63 Cu, 66 Zn, 69 Ga, 72 Ge, 75 As, 78 Se, 85 Rb, 88 Sr, 90 Zr, 93 Nb, 95 Mo, 107 Ag, 111 Cd, 118 Sn, 121 Sb, 125 Te, 133 Cs, 137 Ba, 139 La, 140 Ce, 141 Pr, 146 Nd, 147 Sm, 151 Eu, 157 Gd, 163 Dy, 165 Ho, 166 Er, 169 Tm, 172 Yb, 175 Lu, 178 Hf, 181 Ta, 182 W, 205 TL, 206 Pb, 207 Pb, 208 Pb, 232 Th, and 238 U. Calibration standards for each element listed above were prepared from 0.05 to 200 ng/ml. The internal standard elements used were 6 Li, 45 Sc, 85 Y, 115 In, 159 Tb, and 209 Bi. Calibration standards and samples were analyzed by ICP-MS in triplicate with blanks run every three samples.

3 | RESULTS AND DISCUSSION

3.1 | General results overview

In total, there were one-hundred-eight post-blast samples collected (four replicate shots with twenty-seven samples per shot) and three pre-blast samples for each explosive type (see Table 1). For AN-Al, every sample yielded a measurable amount of aluminum by ICP-MS quantitation from which twenty-seven post-blast and three pre-blast samples were sent for IRMS analysis. For RDX and TNT, recovery was more challenging with only twenty-three post-blast TNT samples (out of 108) and zero post-blast RDX samples yielding a measurable amount of explosive material by HPLC-MS quantitation. RDX and TNT are both high-order explosives, which often result in detonations that consume all or nearly all explosive material. Only three of the samples with detectable TNT yielded enough carbon or nitrogen to measure by IRMS and thus was not included in further analysis.

3.2 | IRMS results for AN-Al

Of the thirty AN-Al samples, data in the form of $\delta^{15}N_{Air}$ (‰) and $\delta^{18}O_{VSMOW}$ (‰) for nitrogen and oxygen, respectively, was acquired for three pre-blast samples and twenty-seven post-blast samples, with one pre-blast sample measured in duplicate. Of the post-blast samples, there were four shots in total with each shot yielding seven, five, five, and six samples, respectively. Shot three had one sample with two technical replicates, and another sample with three technical replicates; the remaining three samples each had one technical replicate. Shot four had one sample with two technical replicates, with the remaining five samples having one technical replicate each. The samples with two or more technical replicates were averaged within each sample and the averages were included back in the data set.

Initial inspection of the scatterplot between oxygen and nitrogen in Figure 2A shows multiple outliers in the post-blast data set. The pre-blast samples (in red) were well-mixed among the post-blast samples (in black). Due to the limited number of samples, Algorithm 1 (see Figure S1) was used on the nitrogen and oxygen measurements individually. Algorithm 1 was performed on the post-blast data only, leaving the pre-blast data to compare with once the analysis was complete. For the atypicality analysis with outlier removal [25–28], the set of hypotheses are as follows:

TABLE 1 Number of post-blast samples analyzed by each technique

Technique	AN-Al	RDX	TNT
Total Recovered	108	108	108
ICP-MS Quantitation	108	N/A	N/A
HPLC-MS Quantitation	N/A	108	108
ICP-MS Profiling	108	N/A	N/A
HPLC-MS Profiling	N/A	0	23
IRMS	27	0	3

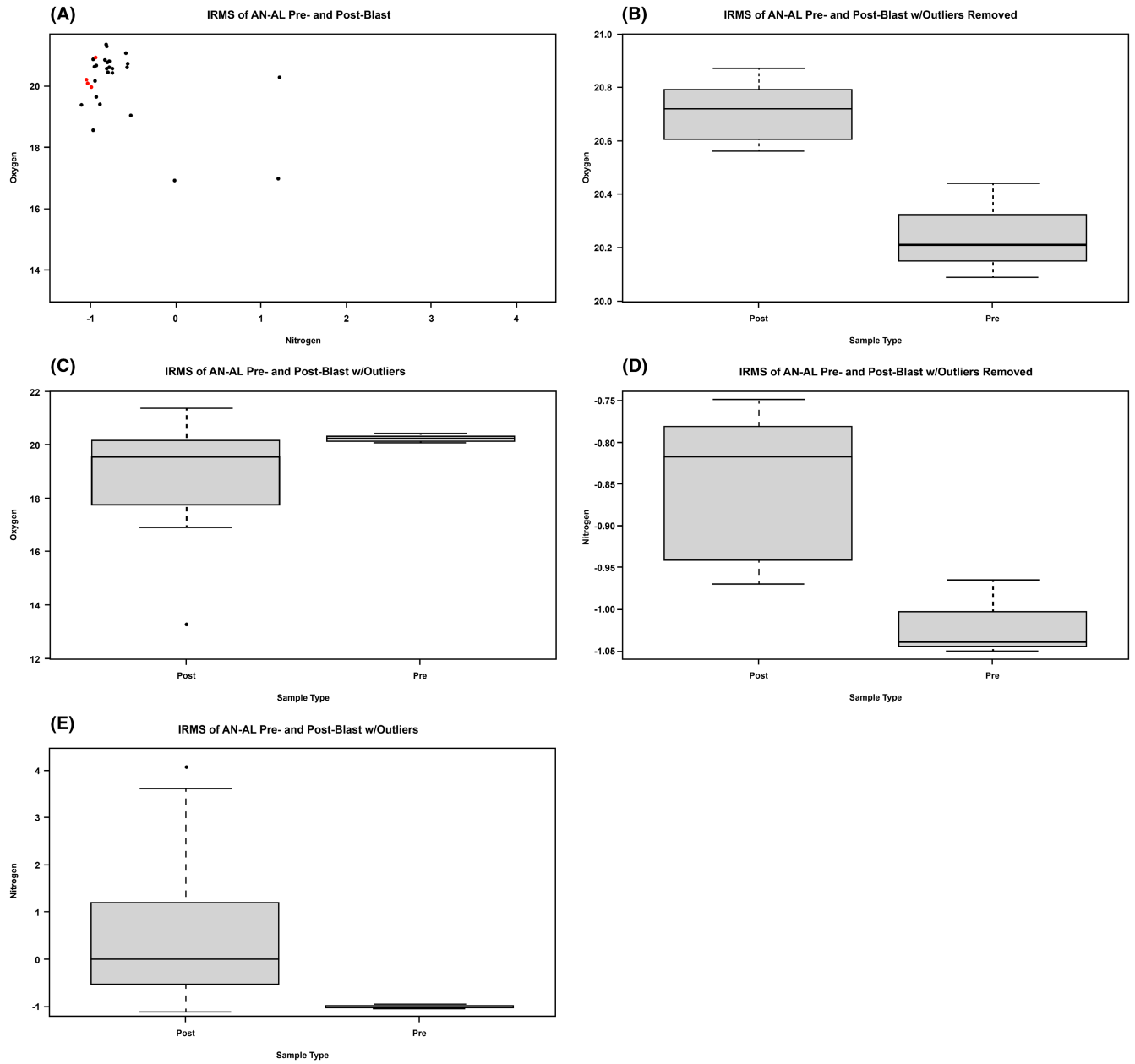

FIGURE 2 (A) Plot of the IRMS technique on AN-Al pre-blast and post-blast data, oxygen (^{18}O) vs nitrogen (^{15}N). Pre-blast measurements are colored red, and post-blast measurements are colored black. (B) Boxplot of the IRMS technique on AN-Al oxygen data comparing post-blast with outliers removed using the atypical analysis, and pre-blast data. (C) Boxplot of the IRMS technique on AN-Al oxygen data comparing post-blast with outliers, and pre-blast data. (D) Boxplot of the IRMS technique on AN-Al nitrogen data comparing post-blast with outliers removed using the atypical analysis, and pre-blast data. (E) Boxplot of the IRMS technique on AN-Al nitrogen data comparing post-blast with outliers, and pre-blast data

- H_0 (the null hypothesis): There is no difference between the removed sample and the average of the remaining sample.
- H_1 (the alternative hypothesis): There is a difference between the removed sample and the average of the remaining sample.

The results of Algorithm 1 on the AN-Al post-blast data are summarized by the boxplots in Figure 2. Figure 2B shows no overlap between the pre-blast oxygen data and the outlier-removed post-blast oxygen data, and Figure 2C shows that the pre-blast oxygen data falls entirely within the interquartile range of the outliers of the post-blast data. Figure 2D shows a small amount of overlap of the interquartile ranges of the boxplots of the pre-blast nitrogen data and the outlier-removed post-blast nitrogen data, and Figure 2E that the pre-blast nitrogen data falls entirely within the interquartile range of the outliers of the post-blast data; note that it falls within the tail of the interquartile range.

For ^{15}N, the standard deviation in the reference material is 0.2‰, so most of the sample distributions overlap within one

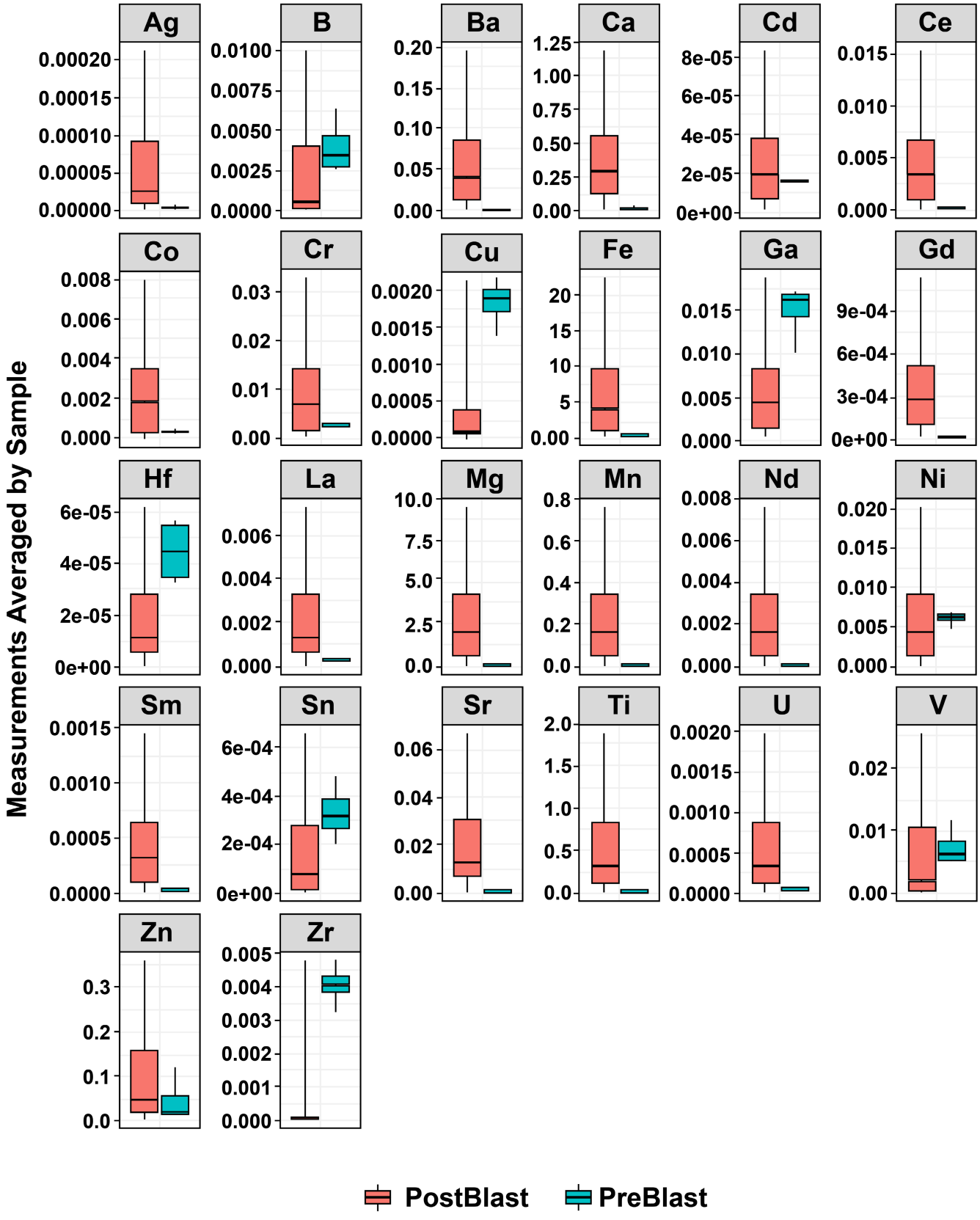

FIGURE 3 Boxplots of the AN-Al blast data measured using the ICP-MS technique. Each element is represented, and the data split into pre-blast and post-blast measurements. The data were averaged across the technical replicates in each sample. Outliers were removed for this plot to better show the range of the boxplots. Outliers were determined by any element measurement greater than the 75th quartile +1.5 * IQR or less than the 25th quartile −1.5 * IQR [Colour figure can be viewed at wileyonlinelibrary.com]

standard deviation of the reference, and the entire spread of the distributions overlap within two standard deviations. Similarly, for ^{18}O, the reference standard deviation is 0.4‰, so the pre- and post-blast distributions partially overlap within one standard deviation, and completely overlap within two standard deviations of the reference. In summary, oxygen and nitrogen isotope ratio results show some overlap between pre- and post-blast for AN-Al when the variability of the IRMS technique is taken under consideration and, therefore, may be useful signatures for attribution.

3.3 | ICP-MS results for AN-Al

Data for all elements measured by ICP-MS was conditioned for statistical analysis in three steps. First, all concentration values that were below three times the limit-of-detection (LOD) were considered not detected and were changed to zero. LOD values can be found in Table S1 of the supplemental. Second, data were blank subtracted by subtracting ten times the average of the blank (for a given element). All subsequent negative values were changed to zero. Third, out of twelve pre-blast sample measurements (four samples with three replicates each), if seven or fewer measurements were below the LOD, the element was removed as a parameter from any further analysis. After applying these conditioning steps, twenty-six elements remained across all AN-Al samples (four replicate detonations each with four pre-blast samples and twenty-seven post-blast samples, all measured in triplicate). The technical replicates were normalized to the Al concentration, and then averaged for all post-blast samples prior to any statistical analysis.

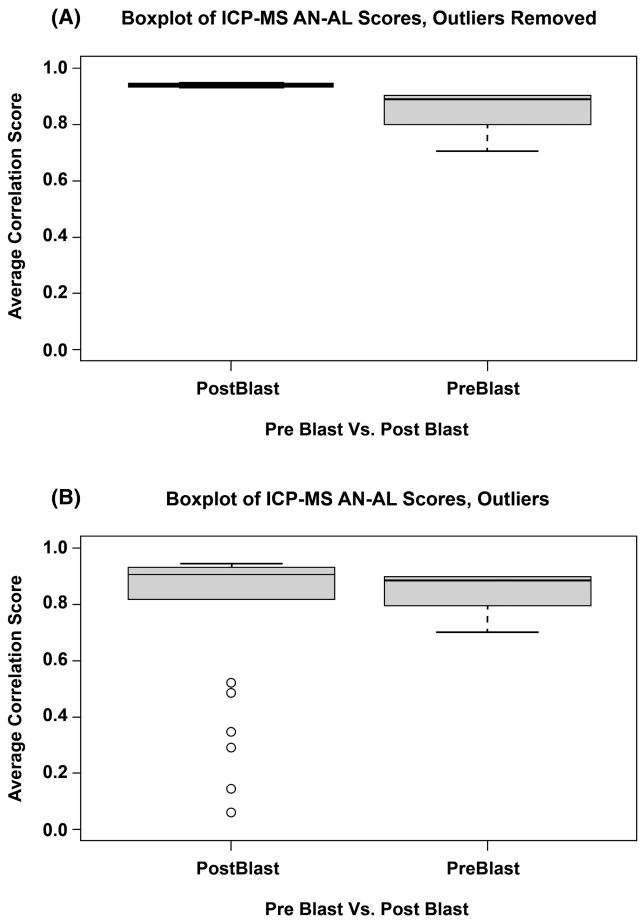

FIGURE 4 (A) Boxplot of the AN-Al blast data measured using the ICP-MS technique. The plot compares the pre-blast scores and the post-blast scores with outliers removed from algorithm 2. (B) Boxplot of the AN-Al blast data measured using the ICP-MS technique. The plot compares the pre-blast scores and the post-blast scores with outliers

Initial inspection of the boxplots in Figure 3, with the outliers (determined by interquartile range (IQR)) removed for visual purposes, shows that the pre-blast samples (in blue) overlap with the post-blast samples (in red) for certain elements, for example, nickel (Ni) and zinc (Zn). Other elements such as copper (Cu) and zirconium (Zr) show little to no overlap between pre-blast and post-blast samples. Algorithm 2 (see Figure S2) was used on all twenty-six elements in conjunction to calculate the cross-correlation scores; it was applied on both the pre-blast and the post-blast data sets separately. This provided a univariate score per sample, reducing the dimensionality allowing for easier visualization. This revealed several outlier samples, so an atypicality analysis [25–28] was conducted to identify and remove outliers from the data. Algorithm 1 was applied to the post-blast cross-correlation scores only, leaving the pre-blast cross-correlation scores to compare with once the analysis was complete.

The results of Algorithm 2 on the AN-Al ICP-MS post-blast cross-correlation scores are summarized by the boxplots in Figure 4. Figure 4A shows the boxplots of the cross-correlation scores of the pre-blast samples and the scores of the post-blast samples with outliers (determined by Algorithm 1) removed. The remaining post-blast scores all had correlations greater than 0.95. In Figure 4B, the post-blast outliers show some overlap between the pre-blast scores and the post-blast outlier scores. These results show promise in the search for a group of elements, B, Cd, Cr, Ni, Sn, V, and Zn in particular, that are consistent pre-blast and post-blast.

4 | CONCLUSION

In this proof-of-concept study, some chemical signatures from pre-blast explosives were shown to be preserved after detonation. While further research and development is required to generate an attribution capability to source an explosive to its manufacturer of origin, this study shows promise that such a capability is possible. This work sought to determine if chemical signatures specific to pre-blast explosive materials could be collected and measured after detonation. IRMS of AN-Al yielded positive results with both oxygen and nitrogen isotope ratios showing some overlap within one standard deviation of the reference between pre- and post-blast samples. Post-blast sourcing of AN-Al was further supported by the results of trace element signatures measured by ICP-MS where the abundances of multiple elements were preserved in both pre- and

post-blast samples. One caveat to be addressed in a potential follow-on study is the inclusion of multiple sources of a single explosive type to determine if the necessary signatures for attribution are preserved after detonation. With this information, combined with the development of a machine learning based sourcing algorithm, a post-blast attribution capability for explosives may be possible in the near future.

FUNDING INFORMATION

This project was supported by National Institute of Justice Interagency Agreement DJO-NIJ-19-RO-0002-2, awarded by the National Institute of Justice, Office of Justice Programs, U.S. Department of Justice. The opinions, findings, and conclusions or recommendations expressed in this publication/program/exhibition are those of the author(s) and do not necessarily reflect those of the Department of Justice. This material is based upon work supported under Air Force Contract No. FA8702-15-D-0001. Any opinions, findings, conclusions or recommendations expressed in this material are those of the author(s) and do not necessarily reflect the views of the U.S. Air Force. Delivered to the U.S. Government with Unlimited Rights, as defined in DFARS Part 252.227–7013 or 7014 (Feb 2014). Notwithstanding any copyright notice, U.S. Government rights in this work are defined by DFARS 252.227–7013 or DFARS 252.227–7014 as detailed above. Use of this work other than as specifically authorized by the U.S. Government may violate any copyrights that exist in this work. Presented at the 73rd Annual Scientific Conference of the American Academy of Forensic Sciences, February 15–19, 2021, held virtually; the 2021 NIJ Annual Forensic Science Research & Development Symposium, February 16, 2021, held virtually; the 2022 NIJ Forensic Science Research & Development Symposium, March 1–2, 2022, held virtually; and at the 2021 Pittcon Conference, March 8–12, 2021, held virtually.

ORCID

Paul Ippoliti https://orcid.org/0000-0001-9795-0202

REFERENCES

1. Gentile N, Siegwolf RTW, Esseiva P, Doyle S, Zollinger K, Delemont O. Isotope ratio mass spectrometry as a tool for source inference in forensic science: a critical review. Forensic Sci Int. 2015;251:139–58. https://doi.org/10.1016/j.forsciint.2015.03.031
2. Nissenbaum A. The distribution of natural stable isotopes of carbon as a possible tool for the differentiation of samples of TNT. J Forensic Sci. 1975;20(3):455–9.
3. Howa JD, Lott MJ, Chesson LA, Ehleringer JR. Carbon and nitrogen isotope ratios of factory-produced RDX and HMX. Forensic Sci Int. 2014;240:80–7. https://doi.org/10.1016/j.forsciint.2014.04.013
4. Benson SJ, Lennard CJ, Maynard P, Hill DM, Andrew AS, Roux C. Forensic analysis of explosives using isotope ratio mass spectrometry (IRMS)—discrimination of ammonium nitrate sources. Sci Justice. 2009;49(2):73–80. https://doi.org/10.1016/j.scijus.2009.04.005
5. Pierrini G, Doyle S, Champod C, Taroni F, Wakelin D, Lock C. Evaluation of preliminary isotopic analysis (C-13 and N-15) of explosives: a likelihood ratio approach to assess the links between semtex samples. Forensic Sci Int. 2007;167(1):43–8. https://doi.org/10.1016/j.forsciint.2006.06.013
6. Gentile N, Siegwolf RTW, Delemont O. Study of isotopic variations in black powder: reflections on the use of stable isotopes in forensic science for source inference. Rapid Commun Mass Spectrom. 2009;23(16):2559–67. https://doi.org/10.1002/rcm.4134
7. Benson SJ, Lennard CJ, Hill DM, Maynard P, Roux C. Forensic analysis of explosives using isotope ratio mass spectrometry (IRMS)-part 1: instrument validation of the DELTAplusXP IRMS for bulk nitrogen isotope ratio measurements. J Forensic Sci. 2010;55(1):193–204. https://doi.org/10.1111/j.1556-4029.2009.01241.x
8. Benson SJ, Lennard CJ, Maynard P, Hill DM, Andrew AS, Neal K, et al. Forensic analysis of explosives using isotope ratio mass spectrometry (IRMS)-part 2: forensic inter-laboratory trial: bulk carbon and nitrogen stable isotopes in a range of chemical compounds (Australia and New Zealand). J Forensic Sci. 2010;55(1):205–12. https://doi.org/10.1111/j.1556-4029.2009.01242.x
9. Brust H, Koeberg M, van der Heijden A, Wiarda W, Mügler I, Schrader M, et al. Isotopic and elemental profiling of ammonium nitrate in forensic explosives investigations. Forensic Sci Int. 2015;248:101–12. https://doi.org/10.1016/j.forsciint.2014.11.024
10. Grimm BL, Stern LA, Lowe AJ. Forensic utility of a nitrogen and oxygen isotope ratio time series of ammonium nitrate and its isolated ions. Talanta. 2018;178:94–101. https://doi.org/10.1016/j.talanta.2017.08.105
11. Barnette JE, Lott MJ, Howa JD, Podlesak DW, Ehleringer JR. Hydrogen and oxygen isotope values in hydrogen peroxide. Rapid Commun Mass Spectrom. 2011;25(10):1422–8. https://doi.org/10.1002/rcm.5004
12. Aranda R, Stern LA, Dietz ME, McCormick MC, Barrow JA, Mothershead RF. Forensic utility of isotope ratio analysis of the explosive urea nitrate and its precursors. Forensic Sci Int. 2011;206(1–3):143–9. https://doi.org/10.1016/j.forsciint.2010.07.030
13. Howa JD, Barnette JE, Chesson LA, Lott MJ, Ehleringer JR. TATP isotope ratios as influenced by worldwide acetone variation. Talanta. 2018;181:125–31. https://doi.org/10.1016/j.talanta.2018.01.001
14. Fraga CG, Mitroshkov AV, Mirjankar NS, Dockendorff BP, Melville AM. Elemental source attribution signatures for calcium ammonium nitrate (CAN) fertilizers used in homemade explosives. Talanta. 2017;174:131–8. https://doi.org/10.1016/j.talanta.2017.05.066
15. Borch T, Gerlach R. Use of reversed-phase high-performance liquid chromatography-diode array detection for complete separation of 2,4,6-trinitrotoluene metabolites and EPA method 8330 explosives: influence of temperature and an ion-pair reagent. J Chromatogr A. 2004;1022(1–2):83–94. https://doi.org/10.1016/j.chroma.2003.09.067
16. Anilanmert B, Aydin M, Apak R, Avci GY, Cengiz S. A fast liquid chromatography tandem mass spectrometric analysis of PETN (Pentaerythritol Tetranitrate), RDX (3,5-Trinitro-1,3,5-triazacyclohexane) and HMX (Octahydro-1,3,5,7-tetranitro-1,3,5,7-tetrazocine) in soil, utilizing a simple ultrasonic-assisted extraction with minimum solvent. Anal Sci. 2016;32(6):611–6. https://doi.org/10.2116/analsci.32.611
17. Avci GFY, Anilanmert B, Cengiz S. Rapid and simple analysis of trace levels of three explosives in soil by liquid chromatography-tandem mass spectrometry. Acta Chromatogr. 2017;29(1):45–56. https://doi.org/10.1556/1326.2017.29.1.03
18. National Academies of Sciences Engineering and Medicine. Existing and potential standoff explosives detection techniques. Washington, DC: The National Academies Press; 2004. p. 56–70.
19. McGuire RR, Velsko CA, Lee CG, Raber E. The use of post detonation analysis of stable isotope ratios to determine the type and production process of the explosive involved. Lawrence Livermore, CA: Livermore National Laboratory; 1993.
20. Telliard WA. Method 1669: sampling ambient water for trace metals at EPA water quality criteria levels. Washington DC: U.S. Environmental Protection Agency; 1996.

21. DeTata DA, Collins PA, McKinley AJ. A comparison of common swabbing materials for the recovery of organic and inorganic explosive residues. J Forensic Sci. 2013;58(3):757–63. https://doi.org/10.1111/1556-4029.12078
22. Hewitt AD. Characterizing range scrap and developing quality assurance coupons for hot gas decontamination trials. JBSA Fort Sam Houston, TX: U.S. Army Environmental Center; 2001.
23. Sigman DM, Casciotti KL, Andreani M, Barford C, Galanter M, Bohlke JK. A bacterial method for the nitrogen isotopic analysis of nitrate in seawater and freshwater. Anal Chem. 2001;73(17):4145–53. https://doi.org/10.1021/ac010088e
24. Casciotti KL, Sigman DM, Hastings MG, Bohlke JK, Hilkert A. Measurement of the oxygen isotopic composition of nitrate in seawater and freshwater using the denitrifier method. Anal Chem. 2002;74(19):4905–12. https://doi.org/10.1021/ac020113w
25. O'Brien A. A kernel based approach to determine atypicality [dissertation]. Brookings, SD: South Dakota State University; 2017.
26. Ausdemore M, Neumann C, Saunders C, Armstrong D, Muehlethaler C. Two-stage approach for the inference of the source of high-dimensional and complex chemical data in forensic science. J Chemom. 2021;35(1):e3247. https://doi.org/10.1002/cem.3247
27. Aitchison J, Dunsmore I. Statistical prediction analysis. Cambridge, U.K.: Cambridge University Press; 1975. https://doi.org/10.1017/CBO9780511569647
28. McLachlan G. Discriminant analysis and statistical pattern recognition. Hoboken, NJ: John Wiley and Sons; 1992.

SUPPORTING INFORMATION

Additional supporting information can be found online in the Supporting Information section at the end of this article.

How to cite this article: Ippoliti P, Werlich J, Fuglsby C, Yarnes C, Saunders CP, Dettman J. Linking ammonium nitrate-aluminum (AN-AL) post-blast residues to pre-blast explosive materials using isotope ratio and trace elemental analysis for source attribution. J Forensic Sci. 2023;68:407–415. https://doi.org/10.1111/1556-4029.15190